

# Integrated Remote Sensing and Machine Learning Dataset of Soil Total Nitrogen in Taiyuan City (2020)

Shao, X.<sup>1,2</sup> Yang, T.<sup>1\*</sup>

1. The CAS Engineering Laboratory for Yellow River Delta Modern Agriculture, Institute of Geographic Sciences and Natural Resources Research, Chinese Academy of Sciences, Beijing 100101, China;  
2. Faculty of Geography, Yunnan Normal University, Kunming 650500, China

**Abstract:** Total soil nitrogen (TN) content is a key indicator reflecting soil nutrient status and ecological functions. Based on the Google Earth Engine (GEE) cloud computing platform, we integrated multi-source remote sensing data and selected key environmental variables—including MODIS-derived NDVI, Sentinel-2 near-infrared reflectance (Band 8), surface soil moisture, precipitation, land surface temperature, and digital elevation model (DEM)—as input features. 3 machine learning algorithms were employed for TN content prediction: Random Forest (RF), Classification and Regression Tree (CART), and Gradient Boosting Regression Tree (GBRT). Using these models, we generated a 2020 soil total nitrogen dataset for Taiyuan City, China. The SoilGrids global soil nitrogen dataset, provided by the International Soil Reference and Information Centre (ISRIC), was used as the reference data. Model performance was evaluated using root mean square error (RMSE) and coefficient of determination ( $R^2$ ) through cross-validation. The average RMSE values for RF, CART, and GBRT across different soil depths were 0.16 g/kg, 0.21 g/kg, and 0.33 g/kg, respectively, with corresponding average  $R^2$  values of 0.62, 0.64, and 0.85. The validation results indicate that the dataset exhibits high accuracy and reliability, providing robust scientific support for regional soil nutrient assessment, agricultural decision-making, and ecological-environmental management. The dataset includes soil total nitrogen content at 6 soil depths (0–5 cm, 5–15 cm, 15–30 cm, 30–60 cm, 60–100 cm, and 100–200 cm) for Taiyuan City in 2020, with a spatial resolution of 30 m. The dataset is archived in .tif format, and consists of 18 data files with data size of 1.52 GB (compressed to 1 file with 219 MB).

**Keywords:** GEE; soil total nitrogen; multi-source remote sensing data; machine learning models

**DOI:** <https://doi.org/10.3974/geodp.2025.03.08>

## Dataset Availability Statement:

The dataset supporting this paper was published and is accessible through the *Digital Journal of Global Change Data Repository* at: <https://doi.org/10.3974/geodb.2025.04.01.V1>.

---

**Received:** 06-05-2025; **Accepted:** 21-07-2025; **Published:** 25-09-2025

**Foundation:** Ministry of Science and Technology of P. R. China (2023YFD1701804)

\***Corresponding Author:** Yang, T., Institute of Geographic Sciences and Natural Resources Research, Chinese Academy of Sciences, yangt@igsrr.ac.cn

**Data Citation:** [1] Shao, X., Yang, T. Integrated remote sensing and machine learning dataset of soil total nitrogen in Taiyuan City (2020) [J]. *Journal of Global Change Data & Discovery*, 2025, 9(3): 323–330. <https://doi.org/10.3974/geodp.2025.03.08>.

[2] Shao, X., Yang, T. A multi-source remote sensing and machine learning integrated dataset of multi-layer soil total nitrogen content in Taiyuan, China (2020) [J/DB/OL]. *Digital Journal of Global Change Data Repository*, 2025. <https://doi.org/10.3974/geodb.2025.04.01.V1>.

## 1 Introduction

Soil serves as the foundation for most terrestrial life, exhibiting unique complexity and dynamic characteristics. Its nutrient composition plays a critical role in maintaining ecological balance and promoting natural development<sup>[1]</sup>. Soil total nitrogen content is a vital indicator for assessing soil nitrogen storage and an essential mineral element for plant growth. It significantly influences soil fertility and vegetation productivity, directly determining crop yield and quality<sup>[2–4]</sup>.

Traditional soil TN monitoring methods primarily rely on field sampling and chemical analysis. While these approaches achieve high precision, they face limitations in sample quantity, temporal cost, and spatial representativeness, making them inadequate for large-scale, high-resolution dynamic monitoring<sup>[5,6]</sup>. With the advancement of remote sensing technologies<sup>[7–9]</sup>, the integration of machine learning models presents a novel approach for constructing regional-scale soil TN content datasets. By synthesizing multi-source remote sensing data and employing nonlinear regression algorithms such as random forest and gradient boosting regression trees, spatial inversion of soil TN content becomes feasible<sup>[5,10]</sup>. These methodologies not only enhance the efficiency and accuracy of soil nitrogen monitoring but also provide scientific foundations for soil management and agricultural decision-making.

The utilization of the Google Earth Engine platform substantially improves computational and temporal efficiency in remote sensing image processing<sup>[11]</sup>, creating opportunities for rapid analysis of massive remote sensing datasets<sup>[12]</sup>. Building upon this framework, this study leverages the GEE cloud computing platform to integrate multi-source remote sensing data with mainstream machine learning algorithms, thereby developing a spatially distributed soil TN content dataset for Taiyuan City in 2020. The dataset encompasses 6 soil layers spanning a depth of 0–200 cm, with a spatial resolution of 30 m, providing foundational support for high-quality cropland resource surveys and regional agricultural information management.

## 2 Metadata of the Dataset

The metadata for the A multi-source remote sensing and machine learning integrated dataset of multi-layer soil total nitrogen content in Taiyuan, China (2020)<sup>[13]</sup> is summarized in Table 1. It includes the dataset full name, short name, authors, year of the dataset, temporal resolution, spatial resolution, data format, data size, data files, etc.

## 3 Methods

### 3.1 Data Sources

(1) NDVI: AVHRR long-term NDVI dataset, 16-day composite, with a spatial resolution of approximately 5.1 km<sup>[15]</sup>; (2) Near-infrared reflectance: Sentinel-2 Level-2A product, Band 8, with a spatial resolution of 10 m<sup>[16]</sup>; (3) Surface soil moisture: OpenLandMap soil moisture at 33 kPa (Band 10), with a spatial resolution of approximately 250 m<sup>[17]</sup>; (4) Precipitation: CHIRPS dataset, 0.05° spatial resolution (approximately 5.6 km)<sup>[18]</sup>; (5) Land surface temperature: MODIS MOD11A1 dataset, daytime LST\_Day\_1 km band, with a spatial resolution of 1 km<sup>[19]</sup>; (6) Digital elevation model (DEM): SRTM DEM dataset, with a

**Table 1** Metadata summary of the A multi-source remote sensing and machine learning integrated dataset of multi-layer soil total nitrogen content in Taiyuan, China (2020)

Items	Description
Dataset full name	A multi-source remote sensing and machine learning integrated dataset of multi-layer soil total nitrogen content in Taiyuan, China (2020)
Dataset short name	TY_SoilN2020
Authors	Shao, X. Faculty of Geography, Yunnan Normal University, 2323130115@ynnu.edu.cn Yang, T., Institute of Geographic Sciences and Natural Resources Research, Chinese Academy of Sciences, yangt@igsrr.ac.cn
Geographical region	Taiyuan City, China
Year	2020
Temporal resolution	Year
Spatial resolution	30 m
Data format	.tif
Data size	1.52 GB (219 MB after compression)
Data files	The soil total nitrogen content for Taiyuan City in 2020
Foundation	Ministry of Science and Technology of P. R. China (2023YFD1701804)
Computing environment	GEE, ArcGIS
Data publisher	Global Change Research Data Publishing & Repository, <a href="http://www.geodoi.ac.cn">http://www.geodoi.ac.cn</a>
Address	No. 11A, Datun Road, Chaoyang District, Beijing 100101, China
Data sharing policy	(1) <i>Data</i> are openly available and can be free downloaded via the Internet; (2) End users are encouraged to use <i>Data</i> subject to citation; (3) Users, who are by definition also value-added service providers, are welcome to redistribute <i>Data</i> subject to written permission from the GCdataPR Editorial Office and the issuance of a <i>Data</i> redistribution license; and (4) If <i>Data</i> are used to compile new datasets, the “ten percent principal” should be followed such that <i>Data</i> records utilized should not surpass 10% of the new dataset contents, while sources should be clearly noted in suitable places in the new dataset <sup>[14]</sup>
Communication and searchable system	DOI, CSTR, Crossref, DCI, CSCD, CNKI, SciEngine, WDS, GEOSS, PubScholar, CKRSC

spatial resolution of 30 m<sup>[20]</sup>; (7) Surface soil nitrogen content: SoilGrids global soil dataset<sup>[21]</sup>.

## 3.2 Algorithm

### 3.2.1 Random Forest Regression

Random Forest (RF) is an ensemble learning method that enhances prediction accuracy by constructing multiple decision trees and aggregating their outputs<sup>[22,23]</sup>. The core idea of RF is to use a “voting” mechanism by training on multiple randomly sampled subsets, thereby reducing the risk of overfitting associated with a single decision tree. In this study, the RF model was trained on integrated multi-source remote sensing data to automatically learn the complex relationships between various environmental factors and soil nitrogen content, ultimately outputting the predicted values of soil nitrogen concentration.

### 3.2.2 Classification and Regression Tree

The Classification and Regression Tree (CART) is a non-parametric statistical method that uses a binary tree structure to split nodes based on specific rules. To enhance prediction accuracy, pruning is applied during the tree-growing process by evaluating subtrees and selecting the final tree that minimizes the average misclassification cost<sup>[24,25]</sup>. Due to its fast implementation, simplicity, and classification accuracy, CART has been widely applied in remote sensing image classification.

### 3.2.3 Gradient Boosted Regression Tree

Gradient Boosted Regression Tree (GBRT) is a boosting algorithm based on decision trees that improves overall model performance by iteratively constructing weak learners and combining their predictions<sup>[26]</sup>. GBRT optimizes model parameters by minimizing a loss function and incrementally adjusting the prediction results to enhance accuracy.

### 3.3 Technical Route

Based on the collection of multi-source data for the year 2020, a series of preprocessing steps were conducted, including data cleaning, format conversion, and spatial resolution harmonization. Subsequently, relevant features were extracted from the preprocessed data, and 3 machine learning models—RF, CART, and GBRT were employed to build prediction models. The selected environmental factors were used as training inputs. Finally, soil total nitrogen content datasets were generated at multiple depth intervals (Figure 1).

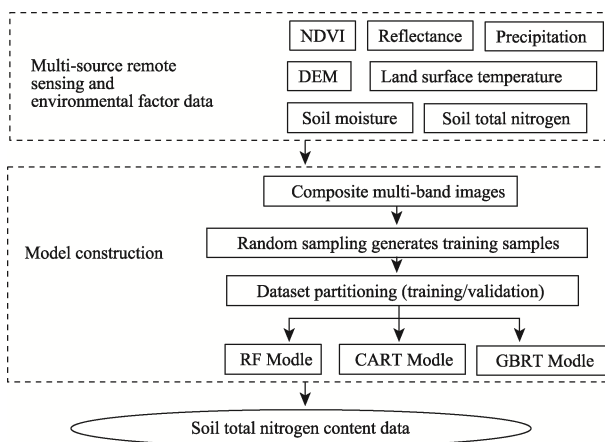


**Figure 1** Flowchart of the dataset development

## 4 Data Results and Validation

### 4.1 Dataset Composition

The dataset is archived in .tif format and consists of 18 data files, corresponding to the outputs of 3 machine learning models: RF, CART, and GBRT for the year 2020 of Taiyuan City. Each model covers 6 soil depth layers: 0–5 cm, 5–15 cm, 15–30 cm, 30–60 cm, 60–100 cm, and 100–200 cm, representing the total nitrogen content in the soil. The spatial resolution of the dataset is 30 m.

### 4.2 Data Results

Figure 2 illustrates the spatial distribution of TN content at multiple depths in Taiyuan City in 2020. Overall, TN content shows a decreasing trend with increasing soil depth. High values are predominantly observed in the surface layer (0–5 cm), while in the deep soil layer (100–200 cm), TN content is generally low, typically below 0.5 g/kg, reflecting the typical pattern of organic matter input and nutrient accumulation at the surface.

Spatially, areas with higher TN content are primarily located in the northern hilly region of Yangqu, the Gujiao mining area, and the mountainous regions of western Lvliang. These

areas are characterized by complex topography, better vegetation coverage, or minimal human disturbance, which contribute to higher accumulation of litter and plant residues—key sources of organic matter and nitrogen. Notably, in the Gujiao mining area, although coal mining has caused localized land degradation, restored vegetation zones exhibit relatively high fertility input. In contrast, areas with low TN content are concentrated in the southern Taiyuan Basin and the Fenhe River Alluvial Plain. These regions are characterized by intensive agricultural activities, where high cultivation intensity and substantial nitrogen loss are prevalent. Additionally, the nitrogen-poor nature of the alluvial parent material and frequent anthropogenic disturbance contribute to the overall low TN levels in these areas.

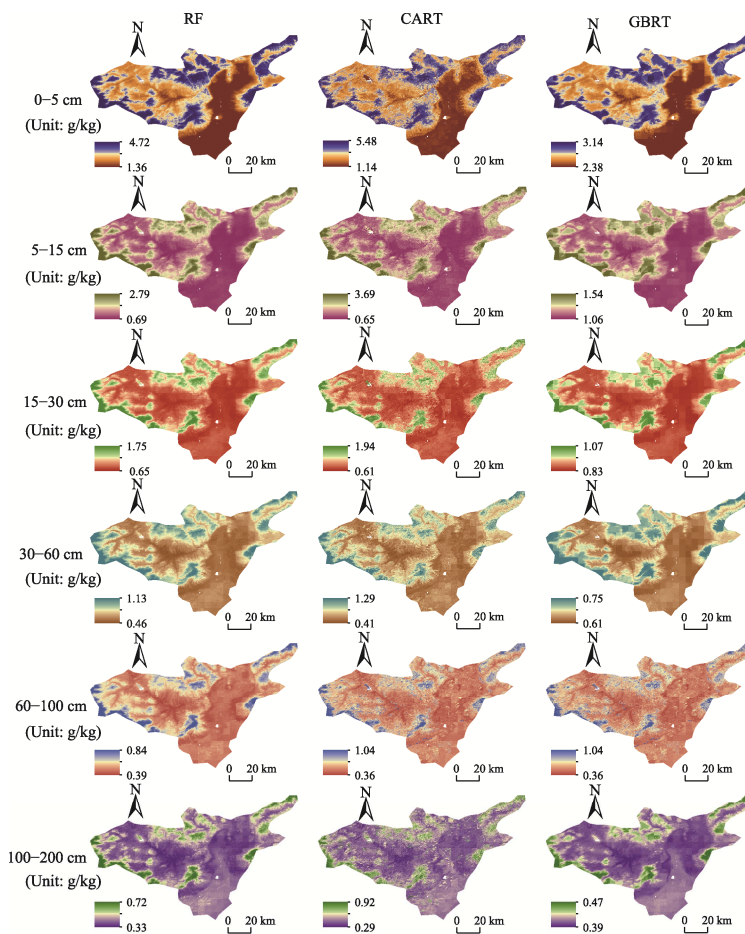


**Figure 2** Spatial distribution maps of multi-layers soil total nitrogen content in Taiyuan City (2020)

### 4.3 Data Validation

To validate the accuracy and reliability of the TN dataset, this study employed the global soil TN data provided by the SoilGrids project of the International Soil Reference and Information Centre (ISRIC) as the benchmark. Cross-validation was conducted, and 2 statistical indicators—Root Mean Square Error (RMSE) and Coefficient of Determination ( $R^2$ )—were used to systematically evaluate and compare the performance of different models across various soil depths. Detailed results are presented in Table 2.

In general, the models exhibited better predictive performance in shallow soils (0–60 cm)

than in deeper layers (60–200 cm), as reflected by higher  $R^2$  values. For instance, in the 0–60 cm depth interval, all models achieved  $R^2$  values exceeding 0.73, indicating a good fit to the spatial variation of TN content at this depth. In contrast, the lowest  $R^2$  dropped to 0.32 in the 100–200 cm layer, indicating a significantly increased prediction error in deeper soils,

**Table 2** Accuracy assessment statistics of the performance of different models

Soil depth (cm)	RF		CART		GBRT	
	RMSE (g/kg)	$R^2$	RMSE (g/kg)	$R^2$	RMSE (g/kg)	$R^2$
0–5	0.40	0.75	0.52	0.75	0.85	0.91
5–15	0.21	0.79	0.28	0.80	0.50	0.91
15–30	0.12	0.73	0.15	0.78	0.26	0.90
30–60	0.08	0.75	0.10	0.77	0.16	0.89
60–100	0.08	0.39	0.10	0.38	0.11	0.76
100–200	0.07	0.32	0.09	0.35	0.10	0.73

likely due to enhanced soil heterogeneity.

Regarding model performance, the 3 machine learning algorithms—RF, CART, and GBRT—showed distinct predictive capabilities across depths and regions. RF demonstrated overall stability, with superior performance in the 0–60 cm range ( $R^2=0.73$ – $0.79$ ), reflecting its robustness to outliers and strong ability to capture complex feature interactions. However, its performance declined markedly in the deep layer (100–200 cm,  $R^2=0.32$ ), indicating limited generalizability. CART showed signs of overestimation in some regions of the surface layer (0–5 cm), where  $R^2$  reached 0.75, but RMSE was as high as 0.52 g/kg, suggesting a risk of overfitting. This may be attributed to CART’s high sensitivity to specific combinations of input variables and its vulnerability to uneven sample distributions or extreme values. GBRT consistently achieved the highest  $R^2$  values across all depths, with powerful performance in the surface layer ( $R^2=0.91$ ). However, the corresponding RMSE reached 0.85 g/kg, indicating “over-responsiveness” to highly variable regions and a tendency to overestimate local TN peaks.

Moreover, differences in variable response mechanisms among models also significantly influenced their predictive performance. CART is more sensitive to high-frequency disturbance variables (e.g., NDVI and land surface temperature), making it prone to extreme value bias. RF tolerates local outliers well but may underestimate local maxima. GBRT, which builds prediction functions through residual-based iterative boosting, excels at capturing complex nonlinear patterns but is sensitive to model parameterization and relies more heavily on terrain-related variables (e.g., DEM), especially in areas with considerable topographic variation.

In conclusion, the 3 models demonstrate varying applicability across different soil depths and geographic regions, underscoring the importance of selecting suitable models based on regional characteristics and specific prediction targets. The soil TN dataset constructed in this study achieved high prediction accuracy in the 0–60 cm layer ( $R^2>0.70$ , RMSE<0.5 g/kg), demonstrating strong scientific applicability and potential for practical use.

## 5 Discussion and Conclusion

This study, based on the Google Earth Engine (GEE) platform, integrated 6 categories of remote sensing data to construct a high-resolution spatial distribution dataset of soil total nitrogen (TN) content in Taiyuan City. Using a regression modeling approach driven by multi-source remote sensing covariates, the dataset achieved a spatial resolution of 30 m. It

significantly improved the representation of soil nitrogen content in complex zones such as agricultural field boundaries (e.g., paddy fields in the Fenhe Plain) and reclaimed mining areas (e.g., the Gujiao mining area). Compared to the global SoilGrids dataset, the results of this study more accurately depict the spatial gradient of soil TN at the regional scale, especially in heterogeneous landscapes characterized by complex land-use structures and strong anthropogenic disturbances. This validates the feasibility and necessity of regional-scale multi-source data fusion modeling.

At the soil profile scale, the TN content in Taiyuan exhibits a pronounced surface-aggregation pattern, with the 0–30 cm layer being significantly enriched, primarily due to surface organic matter input, intensive human activities, and coupled physical-biological processes. In contrast, the TN content decreases progressively with depth, a trend jointly driven by the attenuation of organic input, differentiation of microbial activity, leaching and clay barrier effects, and the depth limitations imposed by root systems and anthropogenic disturbances. This vertical stratification provides theoretical support for controlling non-point source nitrogen pollution and for precise nitrogen application in cultivated areas.

Nevertheless, the dataset has certain limitations. The modeling framework is constrained by single-year observations and the predominance of surface-layer remote sensing covariates, making it difficult to fully capture the physicochemical properties (e.g., pH, cation exchange capacity (CEC), clay content) and interannual dynamics of deeper soil layers. Future work should integrate *in situ* sensor networks, nitrogen cycling process models, and multi-temporal remote sensing data to establish a spatiotemporally continuous soil nitrogen monitoring system encompassing both surface and subsurface layers. Additionally, the incorporation of physically constrained deep learning models is recommended to enhance generalization and transferability in heterogeneous geomorphic regions such as mining areas and alluvial plains.

### **Author Contributions**

Yang, T. designed the algorithms of dataset. Shao, X. collected and processed the multi-source remote sensing data and wrote the data paper.

### **Conflicts of Interest**

The authors declare no conflicts of interest.

### **References**

- [1] Pang, Y. G., Zhang, M. H., Jiang, M., *et al.* Spatial heterogeneity and comprehensive quality assessment of cultivated soil physicochemical properties and microbial characteristics in Gaoyao District, Zhaoqing City, Guangdong Province [J]. *Journal of South China Agricultural University*, 2025, 46(2): 151–163.
- [2] Chapin, F. S., Matson, P. A., Mooney, H. A. Principles of Terrestrial Ecosystem Ecology [M]. Berlin: Springer, 2011.
- [3] Htwe, N. M. P. S., Ruangrak, E. A review of sensing, uptake, and environmental factors influencing nitrate accumulation in crops [J]. *Journal of Plant Nutrition*, 2021, 44(3):1–12.
- [4] Liu, L. Q., Wei, G. Y., Zhou, P. Prediction mapping of soil total nitrogen based on optimized machine learning models using GF-5 imagery [J]. *Smart Agriculture*, 2024, 6(5): 61–73.
- [5] Song, X., Zhang, M., Zhou, H. Y., *et al.* Estimation of soil total nitrogen in Taihu Lake region based on optimized soil spectral parameters [J]. *Journal of Agricultural Resources and Environment*, 2020, 37(1): 43–50. <https://doi.org/10.13254/j.jare.2018.0365>.
- [6] Zhang, H. L., Xie, C. Y., Tian, P., *et al.* Measurement of soil organic matter and total nitrogen using visible/near-infrared spectroscopy and data-driven machine learning methods [J]. *Spectroscopy and Spectral Analysis*, 2023, 43(7): 2226–2231.

- [7] Zhao, C. J. Advances in agricultural remote sensing research and applications [J]. *Transactions of the Chinese Society for Agricultural Machinery*, 2014, 45(12): 277–293.
- [8] Nie, P. C., Qian, C., Qin, R. M., *et al.* Current status and trends of integrated aerial-space-ground information perception and fusion technologies [J]. *Journal of Intelligent Agricultural Equipment*, 2023, 4(2): 1–11.
- [9] Zhang, S., Zhang, J. H., Bai, Y., *et al.* Evaluation and improvement of the daily Boreal Ecosystem Productivity Simulator in simulating gross primary productivity at 41 flux sites across Europe [J]. *Ecological Modelling*, 2018, 368: 205–232. <https://doi.org/10.1016/j.ecolmodel.2017.11.023>.
- [10] Yang, Z., Pan, X., Yuan, J., *et al.* Satellite-based monitoring dataset of cyanobacteria blooms in Lake Taihu (2019) based on random forest algorithm [J]. *Journal of Global Change Data & Discovery*, 2023, 7(3): 321–326. <https://doi.org/10.3974/geodp.2023.03.11>.
- [11] Pan, X. Research on remote sensing image intelligent classification methods of land cover types based on the Google Earth Engine cloud platform [D]. Hohhot: Inner Mongolia Agricultural University, 2021.
- [12] Development and applications of cloud computing platforms for remote sensing in Earth sciences [OL]. <https://d.wanfangdata.com.cn/Periodical/ygxb202101014> (accessed on 13 April 2025).
- [13] Shao, X., Yang, T. A multi-source remote sensing and machine learning integrated dataset of multi-layer soil total nitrogen content in Taiyuan, China (2020) [J/DB/OL]. *Digital Journal of Global Change Data Repository*, 2025. <https://doi.org/10.3974/geodb.2025.04.01.V1>.
- [14] GCdataPR Editorial Office. GCdataPR data sharing policy [OL]. <https://doi.org/10.3974/dp.policy.2014.05> (Updated 2017).
- [15] NOAA National Climatic Data Center. NOAA Climate Data Record (CDR) of AVHRR NDVI, Version 5 [DB/OL]. 2020. [https://developers.google.com/earth-engine/datasets/catalog/NOAA\\_CDR\\_AVHRR\\_NDVI\\_V5](https://developers.google.com/earth-engine/datasets/catalog/NOAA_CDR_AVHRR_NDVI_V5).
- [16] European Space Agency. Sentinel-2 [OL]. <https://scihub.copernicus.eu/dhus/#/home>.
- [17] Hengl, T., Gupta, S. OpenLandMap soil moisture at 33 kPa [DB/OL]. 2017. [https://developers.google.com/earth-engine/datasets/catalog/OpenLandMap\\_SOL\\_SOL\\_WATERCONTENT-33KPA\\_USDA-4B1C\\_M\\_v01](https://developers.google.com/earth-engine/datasets/catalog/OpenLandMap_SOL_SOL_WATERCONTENT-33KPA_USDA-4B1C_M_v01).
- [18] Funk, C., Peterson, P., Landsfeld, M., *et al.* CHIRPS daily precipitation data [DB/OL]. 2015. [https://developers.google.com/earth-engine/datasets/catalog/UCSB\\_CHG\\_CHIRPS\\_DAILY](https://developers.google.com/earth-engine/datasets/catalog/UCSB_CHG_CHIRPS_DAILY).
- [19] NASA. MODIS terra land surface temperature and emissivity daily L3 global 1 km SIN grid V006 (MOD11A1) [DB/OL]. 2020. [https://developers.google.com/earth-engine/datasets/catalog/MODIS\\_006\\_MOD11A1](https://developers.google.com/earth-engine/datasets/catalog/MODIS_006_MOD11A1).
- [20] USGS. SRTMGL1 global 30 m DEM (Version 003) [DB/OL]. 2000. [https://developers.google.com/earth-engine/datasets/catalog/USGS\\_SRTMGL1\\_003](https://developers.google.com/earth-engine/datasets/catalog/USGS_SRTMGL1_003).
- [21] ISRIC—World Soil Information. SoilGrids: global gridded soil information (Nitrogen) [DB/OL]. 2020. [https://developers.google.com/earth-engine/datasets/catalog/projects\\_soilgrids-isric\\_nitrogen\\_mean](https://developers.google.com/earth-engine/datasets/catalog/projects_soilgrids-isric_nitrogen_mean).
- [22] Prasad, A. M., Iverson, L. R., Liaw, A. Newer classification and regression tree techniques: bagging and random forests for ecological regression [J]. *Ecosystems*, 2006, 9(2): 181–199.
- [23] Breiman, L. Random forests [J]. *Machine Learning*, 2001, 45(1): 5–32.
- [24] Wang, D. P., Wang, Z. L., Li, D. Y., *et al.* Classification of desertification land using CART based on integrated non-spectral information [J]. *Journal of Remote Sensing*, 2007, 11(4): 487–492.
- [25] Breiman, L., Friedman, J. H., Olshen, R. A., *et al.* Classification and Regression Trees [M]. Belmont: Wadsworth International Group, 1984.
- [26] Friedman, J. H. Greedy function approximation: a gradient boosting machine [J]. *Annals of Statistics*, 2001, 29(5): 1189–1232.